Effect of Crowding Stress on Lung and Heart of the Adult Albino Rats and the Possible Protective Role of Sulpiride

Tamer M. M. Abu-Amara[1]*, Wagih M. Abdelhay [1], Ayman F. Elsharawy[1], Lotfy S. Mohamed[1], Salah E. Mourad[2], Abdelghany H. Abdelghany[3] and Neama M. Taha[4].

[1]Histology&Cytology Department, Faculty of Medicine, Al-Azhar University, Cairo, Egypt.
[2] Anatomy & Embryology Department, Faculty of Medicine, Al-Azhar University, Cairo, Egypt.
[3]Anatomy & Embryology Department, Faculty of Medicine, Alexandra University, Egypt.
[4]Physiology Department, College of Medicine, Umm Al-Qura University, KSA.
*Corresponding author: Tamer M. M. Abu-Amara, Lecturer of Histology & Cytology Department, Faculty of Medicine, Al-Azhar University, Egypt, E-mail: tamer4567@yahoo.com

Abstract: Exposure to crowding stress is associated with increased respiratory system morbidity, However, the underlying mechanisms are unclear. Thus, there is a need for more study of this harmful effect. Sulpiride had been shown to have a protective role against crowding stress on other systems but this role was not studied well on the respiratory and cardiovascular systems.
Objectives: Investigating the possible harmful effects of crowding on adult albino rats' lung and heart and the possible protective role of combined sulpiride treatment.
Materials and Methods: The present study was carried out on 24 adult albino rats of local strain weighing 120±3 g which were randomly divided equally into **Group 1(C, untreated negative control), Group 2 (Cr, crowding exposed or positive control)** where rats were exposed to crowding in a cage (20x20x20 cm- 6 rats /cage) for 1 month**, Group 3(D, sulpiride-treated)** where the rats were exposed to sulpiride "0.028 mg/B.W./day" and **Group 4 (Cr+D, crowding + sulpiride-treated).** Paraffin sections were prepared for histological, histochemical and morphometric studies. The data were statistically analysed.
Results: The rats exposed to crowding only or sulpiride only showed highly significant damaging changes on lung such as thickening in the interalveolar septa and obliteration of the alveoli, inflammatory cells infiltration within the pulmonary interstitium, peribronchiolar infiltration and fibrosis, thickening of the pulmonary blood vessels walls, interstitial collagen fibres deposition and apoptotic cellular changes. On the level of heart, significant decrease in the diameters of the myocardial muscle fibres with focal areas of necrosis, apoptotic changes and increased collagen fibres deposition was marked in sulpiride group. When crowding and sulpiride treatments were combined, the damaging effects were maximized on the lung and heart.
Conclusion: These results provided evidence that crowding stress causes obvious lung and heart tissue damages. No protective role for sulpiride was proofed. This is because using sulpiride alone or in combination with crowding showed marked damaging effects on the lung and heart tissues.
Keywords: Crowding, Sulpiride, Lung, Heart, Stress, Histology and Histochemsitry.

Introduction

Crowding stress is a type of psychosocial stress induced by an increased density of population. Population density may be raised either by increasing the number of species living in the same area and/or by reducing their living space[(1)]. Crowding stress induces complex changes at the behavioural, physiological and molecular levels with subsequent serious social, medical, economic and environmental implications[(2,3)]. Environmental changes related to crowding particularly in small limited spaces include increasing temperature hypoxia, change of air humidity considered as a risk factor that increases the mortality rate due to respiratory tract infection especially among infants[(4)]. This interferes with personal activities leading to antisocial behaviour[(5)]. For instance, crowding was found as an important factor related to poor school performance of children[(6)]. Crowding could be seen as a social condition of high interpersonal situation where it involves an unwanted, unnecessary or interfering potential or actual interaction without real high density of population[(7)]. Exposure to

DOI: 10.12816/0008490

crowding has been reported to affect pituitary adrenal axis activity with increased plasma ACTH and corticosterone with heavier adrenal than normal[8]. Crowding may also cause alteration of the neuroendocrine control of growth hormone (GH), thyroid-stimulating hormone (TSH) and serum insulin hormone[9]. Crowding may affect behaviour by increasing plasma free tryptophan level and increased brain level of tryptophan and serotonin[8]. Crowding may result in harmful physical and mental diseases with deterioration of human function. The hormonal changes which occur during crowding may result in metabolic changes and it may act synergistically with other substances to promote some metabolic diseases such as diabetes mellitus, atherosclerosis, and heart diseases[5]. Prolonged exposure to crowding is associated with withdrawal, from interaction, poor health, crime, and aggression[3].

Antidepressant drugs are the most successful in patients with clearly (vegetative) characteristics including psychomotor retardation, sleep disturbance, poor appetite and weight loss. However, a variety of chemical structures has been found to have antidepressant activity[9]. Sulpiride "a neuroleptic drug" from the group of benzamides exerts antiautistic stimulating effects, has positive influence on productive symptoms of psychosis and shows antidepressant activity[10,11,12,13,14]. Sulpiride is the most favorite drug which is used to tolerate stress symptoms as it has relatively minor adverse effects [10]. Also, in comparison to many tricyclic antidepressant, sulpiride reaches its maximal blood concentration after 2-4 hours from oral administration[15,16,17]. This work was done using histological, histochemical and morphometric methods to investigate two parameters; the first parameter was to investigate the possible harmful effects of crowding on the adult female albino rats' lung and heart; and the second parameter was to investigate the possible protective role of combined sulpiride treatment.

Materials and Methods

Animals: Twenty four adult albino rats weighing 120±3 g were used in this study. They were kept under observation for one week before beginning of the experiment to acclimatize. During every day, the animals were exposed to 14 hr artificial light followed by 10 hr complete darkness at normal room temperature. All the animals were fed on standard diet contained protein, fibres, fats, carbohydrates, and supplied with vitamins, minerals mixture and water. Sulpiride drug was adiministrated orally by gastric tube at a dose of 0.28mg/ 100 g body weigh/day for one month. Sulpiride dose was calculated according to the Paget's formula on the basis of the human dose[18]. Crowding was applied by putting rats in a cage (20x20x20 cm - 6/cage).

Study groups: The animals were divided into four equal groups. **Group 1 (C):** The rats were served as negative control (without any treatment for one month). **Group 2 (Cr):** The rats were exposed to crowding in a cage (20x20x20 cm – 6 rats/cage) for one month. **Group 3 (D):** The rats were treated with the drug only for one month (0.028mg/g body weigh /day). **Group 4 (Cr+D):** The rats were exposed to crowding (20x20x20 cm-6 rats /cage) and treated daily with the drug for one month.

Histological and histochemical study: The rats of the control and treated groups were sacrificed after one month and small pieces of lung and heart were taken for the histological and histochemical studies. Specimens were prepared via fixation in 10% neutral buffered formalin solution and Carnoy's fluid. Paraffin sections of 5µm thickness were prepared and stained with Harris haematoxylin and eosin[19]. The collagen fibres were stained by using Mallory's trichrome stain[20]. The polysaccharides were detected by PAS (Periodic acid-Schiff) method[20].

Morphometric analysis: The image analyzer (ImageJ 1.46r) was used to obtain the following morphometric data:

- The mean thickness of the interalveolar septa using H&E- stained sections at 400x magnification.
- The mean number of the alveolar macrophages/field using oil immersion lens in H&E-stained sections at 1000x magnification.
- The area percentage of the collagen fibres in the lung alveoli using Mallory's

trichrome-stained sections at 400x magnification.

- The mean thickness of the pulmonary vessels in the lung interstitium using H&E-stained sections at 400x magnification.
- The mean thickness of the cardiac myocytes using H&E-stained sections at 400x magnification.
- The area percentage of the collagen fibres in the cardiac myocytes using Mallory's trichrome-stained sections at 400x magnification. The previous measurements were estimated in five non-overlapping fields/section in five serial sections/rat from each animal in each group.

Statistical analysis: All statistical analyses were performed *via* **PAleontological Statistics Version 3.0 (PAST 3.0) statistical software *(*Hammer *et al., 2001)*[21]**. The obtained data were expressed as mean ± standard deviation (SD) and analyzed using analysis of variance (ANOVA). Statistical significance level was defined as $p<0.05$.

Results

The control group, Group 1 (C): H&E-stained sections of the lung tissue showed normal alveoli with thin interalveolar septa, clearly seen alveolar sacs, bronchioles with folded lining of columnar epithelial cells and normal pulmonary blood vessels **(Figs. 1A, 2A)**. The alveolar epithelium showed type I pneumocytes (extremely flattened with very thin cytoplasm and densely-stained flattened nuclei) and type II pneumocytes (cuboidal cell with large darkly-stained spherical nuclei which are commonly located near the angles between neighbouring alveolar septa) **(Fig. 3A)**. Little number of macrophages was also detected in the lung interstitium **(Fig. 3A)**. Within **group 1,** Mallory's trichrome-stained sections of lung tissue revealed normal distribution of thin collagen bundles in pulmonary interstitium around the alveolar sacs, in the interalveolar septa, around bronchioles and the pulmonary blood vessels **(Fig. 4A)**. In **group 1,** Periodic acid-Schiff (PAS)-stained sections of the lung tissue showed moderate PAS +ve reaction (magenta red) in the basal lamina of the alveolar epithelium, alveolar sacs and endothelium of pulmonary vessels as well as cytoplasm of epithelium lining bronchioles **(Fig. 5A)**. **Group 2 (Cr) and Group 3 (D):** H&E-stained sections of the alveolar tissue showed obliteration of some alveoli with subsequent compensatory dilatation of others **(Figs. 1B, 2B, 1C, 2C)**. Within **Group 2**, significant increase in thickness of the interalveolar septa ($p< 0.05$) was detected **(Figs. 1B, 2B, 10 and Table 1)**, while in **group 3,** there was highly increased thickness of the interalveolar septa ($p< 0.001$) **(Figs. 1C, 2C, 10 and Table 1)**. In both **groups (2&3)**, there were cellular apoptotic changes such as pyknotic nuclei in the lung interstitial cells **(Figs. 3B, 3C)**. Also, there was a highly-significant increase in both inflammatory cells infiltration within connective tissue surrounding lung bronchioles ($p< 0.001$) and pulmonary blood vessels diameter ($p< 0.001$) **(Figs. 1B, 2B, 1C, 2C, 12, 13 and Table 1)**. Mallory's trichome-stained sections of the lung tissue of **group 2** showed significant deposition of collagen fibres ($p< 0.05$) in bronchiole walls, peribronchiolar areas, interalveolar septa, and pulmonary blood vessels **(Figs. 4B, 11 and Table 1)**. While **group 3** showed highly significant deposition of collage fibres ($p< 0.001$) in bronchiole walls, peribronchiolar areas, interalveolar septa, and pulmonary blood vessels **(Figs. 4C, 11 and Table 1)**. PAS-stained sections of the lung tissue of **group 2** revealed strong PAS+ve reaction in RBCs seen in the congested pulmonary vessels, endothelium of the pulmonary vessels, inflammatory cells infiltration, shedded bronchiole epithelial cells and in sites of interstitial cellular infiltration. Also, strong PAS+ve reaction in alveolar epithelium, alveolar sacs and collapsed alveoli were observed in **group 2 (Fig. 5B)**. **Group 3** illustrated similar findings to crowding exposed one. However, weak PAS+ve reaction was observed in the perivascular areas and collapsed alveoli in **group 3 (Fig. 5C)**. **Group 4 (Cr+D):** H&E-stained sections of the lung tissue showed marked obliteration of some alveoli with subsequent compensatory dilatation of others and thickened interalveolar septa. **(Figs. 1D, 2D, 10)**. Moreover, marked thickening of the bronchiole walls and peribronchiolar infiltration with inflammatory cells were detected. Highly

significant thickening of pulmonary blood vessels ($p< 0.001$) was detected with marked perivascular infiltration and degeneration **(Figs. 1D, 2D, 13 and Table 1)**. Furthermore, more necrotic tissue and cellular pyknotic changes than **groups 2 & 3** had been shown in **group 4 (Fig. 3D).** Also, high significant increase in both cellular infiltration within the connective tissue surrounding lung bronchioles and increase in the pulmonary blood vessels thickness ($p< 0.001$ and < 0.001 respectively) were also detected **(Figs. 1D, 2D, 12, 13 and Table 1)**. Within **group 4,** Mallory's trichome-stained sections of the alveolar tissue revealed marked highly significant increase in collagen fibres deposition ($p< 0.001$) in bronchiole epithelial cells, submucosa, peribronchiolar area, in thick interalveolar septa and around the pulmonary blood vessels with marked thickening of their walls **(Figs. 4D, 11 and Table 1)**. In **group 4**, PAS-stained sections of the alveolar tissue showed very strong PAS+ve reaction in endothelium of the pulmonary vessels, in perivascular areas, and in sites of interstitial cellular infiltration, peribronchiolar areas and collapsed alveoli **(Fig. 5D).**

The control group, Group 1 (C): H&E-stained sections of the cardiac muscle fibres illustrated branching and anastomosing cardiac muscle fibres with acidophilic sarcoplasm and central elongated vesicular nuclei of cardiomyocytes and the nuclei of fibroblasts in the interstitium **(Figs. 6A, 7A)**. Also, Mallory's trichrome-stained sections of the cardiac muscles revealed few collagen fibres in-between the muscle fibres **(Fig. 8A)**. Furthermore, PAS-stained sections of the cardiac muscle revealed normal polysaccharides' content (normal distribution of PAS+ve materials) in the cardiac tissue **(Fig. 9A)**. **Group 2 (Cr) and Group 3 (D):** H&E-stained sections of the cardiac muscle fibres of **group 2** illustrated some degenerative changes of the myocardial muscle fibres **(Fig. 6B)**. **Group 3** showed cardiac myocytes degenerative changes **(Fig. 6C)**. Focal areas of necrotic muscle fibres with vacuolated cytoplasm, small deeply-stained pyknotic nuclei and faintly-stained karyolytic nuclei were detected in both **groups 2 & 3 (Figs. 7B, 7C)**. Within **group 3,** a significant decrease in the diameter of myocardial muscle fibres ($p< 0.05$) was detected **(Fig. 14 and Table 1)**. Mallory's trichrome-stained sections of the cardiac muscle fibres of both **groups (2 & 3)** showed highly-significant increase of the collagen muscle fibres deposition ($p< 0.001$) in comparison to the control group **(Fig. 8B, 8C**, **15 and Table 1)**.

In addition, PAS stained cardiac muscle fibres of **groups 2 & 3** revealed poorly stained (focal areas of decreased staining affinity of PAS stain) cardiac myocytes **(Figs. 9B**, **9C).**

Group 4 (Cr+D): H&E-stained sections of the cardiac muscle fibres showed marked myocardial cellular degenerative changes **(Fig. 6D)**. More necrotic areas with vacuolated cytoplasm and small deeply-stained pyknotic nuclei than both **groups (2 & 3)** were detected **(Fig. 7D)**. Highly-significant decrease in the diameter of the myocardial muscle fibres within **group 4** ($p< 0.001$) was detected **(Fig. 14 and Table 1)**. Within **group 4**, Mallory's trichrome-stained sections of the cardiac muscle fibres revealed marked highly-significant deposition of collagen fibres ($p< 0.001$) in bronchiolar epithelial cells, submucosa, peribronchiolar area and in thick interalveolar septa with cellular infiltration in interalveolar septa **(Figs. 8D, 15 and Table 1)**. Also, PAS-stained sections of the cardiac muscle fibres showed poorly-stained (focal areas of decreased staining affinity of PAS stain) cardiac myocytes **(Fig. 9D).**

Discussion

Crowding stress had been shown to carry many negative drawbacks on various organs of our body[2,3]. Crowding affects individuals either directly or indirectly by the associated conditions[6]. The environmental changes related to crowding such as increasing temperature, hypoxia, change of air humidity are considered as risk factors that increases the mortality rate due to respiratory tract infection especially among infants[4]. Exposure to crowding has been reported to affect pituitary adrenal axis activity with increased plasma ACTH and corticosterone, hyperactivity of sympathetic adreno-medullary system with increased adrenaline and noradrenaline

secretion[1,3,8]. Moreover, crowding may alter the neuroendocrine control of the growth hormone (GH), thyroid stimulating hormone (TSH) and serum insulin[8]. Stress can cause hypertension and subsequent congestive heart failure *via* its damaging effects on kidney[22,23]. Also, mechanical stress increases reactive oxygen species (ROS) production that leads to cardiomyocytes apoptosis and subsequent heart failure[24,25]. Liver injury, inflammation and fibrosis after exposure to stress were reported[26]. Our study showed that crowding stress and sulpiride treatment caused remarkable histological and structural drawbacks on lung and heart tissues. Rats exposed to crowding only or sulpiride only showed highly significant damaging changes in the lungs such as thickening in the interalveolar septa and obliteration of alveoli, inflammatory cells infiltration within pulmonary interstitium, peribronchiolar infiltration and fibrosis, thickening of the pulmonary blood vessels, interstitial collagen fibres deposition and apoptosis. ***Tamer et al.***[27] study showed almost similar effect for noise stress alone and in combination with sulpride treatment on lung tissue in adult albino rats. On the level of heart, highly significant decrease in the diameter of myocardial fibres with focal areas of necrotic fibres and apoptotic changes were detected. Also, collagen fibres deposition was marked in sulpiride group. When crowding and sulpiride treatment was combined, the damaging effects were maximized on the lung and to a lesser extent on the heart. ***Tamer et al.*** [27] study showed almost similar effect for noise stress alone and in combination with sulpride treatment on heart tissue. ***Eman et al.***[28] study showed similar effect for noise stress on kidney cortex, where highly thickened arterial walls and increased Kupffer cells were detected. In our study, the increased number of inflammatory cells may be due to and reflecting the active defence mechanism against the crowding stress or the toxic effect of sulpiride. ***Maisa***[29] study showed similar results for crowding stress that lead to necrosis and ulceration of the gastric mucosa in adult albino rats. ***Zhang & Kaufman***[23] declared that increasing Kupffer cells' numbers may reflect the active defence mechanism against the toxic substances. Increased collagen fibres observed in our current study may lead to rapid healing as reported by ***Zhang et al.***[30]. The increase in collagen fibres deposition under different stresses was observed by several authors[31,32,33,34]. In this issue, **George *et al.***[35] suggested that decreased synthesis of collagenolytic enzymes that might contribute to further accumulation of collagen. Thickened arterial walls observed in our study were also detected by other authors[22,28,36]. Exposure to stress induces oxidative stress leading to increased free radical production which cause hypertrophy of both vascular smooth muscle fibres and arterial walls hypertrophy[22,36]. Alerted collagen fibres and polysaccharides in the present study may be a result of elevated free radicals post-exposure to stress as seen in previous studies[24,37]. Also, decreased protein content after exposure to other kinds of stress was detected in brain in previous studies[24,37]. In this issue, ***Willis et al.***[38] showed that stress inhibits protein synthesis via altering the balance between phosphorylation and dephosphorylation. Moreover, increased protein breakdown had been detected after acute induction of corticosteroids to normal fasting humans[39]. Protein degeneration that was noticed in other studies is properly due to injury of mitochondria, Golgi apparatus and DNA fragmentation[33,40,41]. Different kinds of stressors can affect mitochondria leading to rupture of the outer mitochondrial membrane, release of the inner membrane components, apoptosis and finally induce cell death[42,43]. Similar to the related previous studies, the histological changes of our study may result from an increase in the lipid peroxidation process or decreasing in the antioxidant enzymes activity of the body with the consequent damage of the cell membranes[44,45]. The beneficial effects of sulpiride in treating some disorders were reported by several authors[46,47,48]. Also, previous studies such as that of ***Eman et al.***[28] showed that sulpiride drug may have a protective role against stress negative drawbacks. However, our results showed that sulpiride has a harmful effect on the lung and heart tissues when it was used alone or in combination with crowding.

In conclusion, our results provide evidence that crowding stress causes noticeable lung and heart tissue damages. No protective role for sulpiride was proofed as using sulpiride showed marked damaging effects on the lung and heart.

References

1. **Eva V, Harald G, Ellen M and Svein O (2010):** Cangesin muscle and blood plasma proteomes of atlantic salmon induced by crowding. Journal of Aquaculture. **132**:272-279.
2. **Benyo Z, Szabo C and Kova AP (2007)**: Prevention of the hemorrhagic hypotension-induced hepatic arterial vasoconstriction by L-arginine and naloxone. Shock. **11**: 342–346.
3. **Lorenz HF, Terence I, Walker R and Richared D (2010):** Trawal capture of part Jackson sharks, heterdontus and gummy sharks. Mustelus antarcticus incontroled settiowding :effect of low duration , air exposure and crowding. Fisheries Research. **106**:344-350.
4. **Frank T (2010):** Cultures as problem in linking material in equality to health: on residential crowding. Journal of Pharmacology, Biochemistry and Behavior. **16**: 523- 530.
5. **Hoon L and Alan R (2003):** Crowding at an arts festival: extending crowding models to the front country. Journal of Tourism Management. **24**: 1-11.
6. **Maltos E, Tome S, Silva T and Maria D (2011):** Effect of harvesting stress and storage conditions on protein degradation in fillets of formed gilthead sea bream: A differential scanning calorimetry study. Food Chemistry. **126**:270-276.
7. **Ganga R, Montero D, Juan M and Eneko G (2011):** Stress response in sea bream (*Sparus aurata)* held crowded conditions and fed diets containing linseed and /or soybean oil. Journal of Agriculture. **311**: 215-223.
8. **Thomas JK and Janz DM (2011):** Dietary selenomethionin exposure in adult zebrafish alters swimming performance, energetic and the physiological stress. Journal of Aquacultue. **304**:104-107.
9. **Rosana C, Tania M, Elizabeth M and Yonamine MC (2010):** Ethanol-induced sensitization depends preferentially on D_1 rather than D_2 dopamine receptors. Pharmacology, Biochemistry and Behavior. **98**: 173-180.
10. **Jae-Jin K, Dae J, Tae-Gyun K, Jeong-Ho S and Ji–Won C (2007):** Volumetric abnormalities in connectivity based subregions of the thalamus in patients with chronic schizophrenia. Schizophrenia Research. **97**: 226-235.
11. **Charles E (2011):** Psychopharmacology: house divided .progress in neuro-psychopharmacology and biology. Journal of Psychiatry. **35**:1-10.
12. **Camarini R, Marcorkis T, Teodorv E and Maria H (2011):** Ethanol-induced sensitization depends preferentially on D1 rather than D2 dopamine receptors. Journal of Schizophrenia Research, **97**: 226-235. Biochemistry and Behavior. **98**: 173-180.
13. **Mohammad N, Fatemeh M, Shahrbanoo O, Sima N and Mohammad R (2011):** The effects of dopaminergic drugs in the dorsal hippocampus of mice in the nicotine-induced anxiogenic-like response. Pharmacology, Biochemistry and Behavior. **98**: 468-473.
14. **Mori K, Kim J and Sasaki K (2011):** Electrophysiological effects of orexin–B and dopamine on rat nucleus accumbens shell neurons *in vitro*. Peptides. **32**: 246-252.
15. **Nikol F, Mira S and Christos R (2005):** Canine versus in vitro data for predicting input profiles of 1-sulpiride after oral administration. European Journal of Pharmaceutical Sciences. **26**: 324-333.
16. **Michal A and Ina W (2008):** Fluctuation of latent inhibition along the estrous cycle in the rat: modeling the cylicity of symptoms in schizophrenic women. Journal of Psychoneuroendocrinology. **33**: 1401-1410.
17. **Martin S, Cindy L and Stephan F (2010):** Cholineric contribution to the cognitive symptoms of schizophrenia and the viability of cholinergic treatment. Journal of Schizophrenia Research, **97**: 226-235. Journal of Neuropharmacology. **34**: 188-195.
18. **Paget GE and Barnes JM (1964):** Evaluation of drug activityIn**:** Pharmaceutics Laurence and Bacharach, Vol.1 Academic press, NewYork.
19. **Drury R and Wallington E (1980):** Carleton's Histological Technique. 4th Ed. Oxford. Univ. Press, New York, Toronto, Pp: 115-119.
20. **Pearse A (1977):** Histochemistry, Theoretical and Applied. 3rd Ed vol I**.** Churchill Livingstone, London, Pp: 112-115.
21. **Hammer Ø, Harper DAT and Ryan PD** (2001). PAST: Paleontological Statistics Software Packagefor Education and Data Analysis. Palaeontologia Electronica, **4**(1): 9-15.
22. **Agarwal MD (2005)**: Hypertension in chronic kidney disease and dialysis: pathophysiology and management. Cardiol. Clin, **23**: 237-248.
23. **Zhang K and Kaufman RJ (2008):** From endoplasmic–reticulum stress to the inflammatory response. Journal of Nature, **454**: 455-462.
24. **Samson T, Sheela D, Ravidran M and Senthilvelan A (2005):** Effect of noise stress on free radical scavenging enzymes in brain.

Environmental toxicology and Pharmacology, **20**:142-148.

25. **Katzung BG (2008)**: Basic and Clinic Pharmacology, Appleton and Lange, Lebanon, Pp: 448–460.
26. **Vere CC, Streba T and Ionescu G (2009):** Psychosocial stress and liver disease status**.** World Gastroenterology. **28**:2980-2986.
27. **Tamer MMAbu-A, Gamal SE, Moustafa EEM, Salah EM, Neama MT (2013):** Effect of Noise Stress on Lung and Heart of the Adult Albino Rats and the Possible Protective Role of Sulpiride The Egyptian Journal of Hospital Medicine. **53**:1083– 1105.
28. **Eman GH, Fatma E and Neama MT (2011).** Protective effects of sulpiride treatment on kidney functions of female albino rats exposed to noise stress. The Egyptian Journal of Hospital Medicine. **44**: 284 – 294.
29. **Maisa MAAl-Q (2012)**: Effect of the Overcrowding Stress on Fundus of Stomach in Adult Male Albino Rats. Current Research Journal of Biological Sciences. **4**(4): 482-487.
30. **Zhang D, Xu Z, Chiang A, Lu D and Zeng Q (2006):** Effect of GSM 1800 MHz radiofrequency EMF on DNA damage in Chinese hamuster lung cells. Zhonghuo Nei. Brain Research. **916**: 107–114.
31. **Shediwah F (2005):** Control of toxicity induced during chemotherapy and radiotherapy using natural plant substance. Ph. D. Thesis, Zoology Department, Faculty of Science, Al-Azhar Univ, Cairo.
32. **Al Gahtani S (2006):** Histological and histochemical studies on the effect of two different types of magnetic field on the liver and kidney of albino rats. M.Sc. Zoology Department, Girls College of Science, Dammam, K.S.A.
33. **Eid F and Al-Dossary A (2007):** Ultrastructural, histological and histochemical studies on the effect of electraomagnetic field on the liver of pregnant rats and their fetuses. The Egyptian Journal of Hospital Medicine. **28**: 273-294.
34. **El Salkh B (2009):** Histological and histochemical studies on the effect of the alternating magnetic field on the mice lung. Egypt. Journal of Schizophrenia Research, **97**: 226-235. Journal of Biomedical Science. **29**: 351-366.
35. **George I, Ramesh k, Stem R and Chandrakasan G (2001)**: Dimethyl nitrosamine-induced liver injury in rats: the early deposition of collagen. Journal of Toxicology. **156**: 129-138.
36. **Gu JW, Anand V and Shek EW (1998):** Sodium induces hypertrophy of cultured myocardial myoblasts and vascular smooth muscle cell. Journal of Hypertension. **31**:1083-1087.
37. **Nikolaos P, George Z, Nikolaos TP, Christos DG, Fevronia A and Nikolaos AM (2004):** Thiol redox state (TRS) and oxidative stress in the mouse hippocampus after pentylenetetrazol-induced epileptic seizure. Neurosci. Lett. **357**: 83-86.
38. **Willis C, Armario A and Piganini H (2009):** Cholesterol and triglyceride concentration in rat plasma after stress. Pharmacol. Biochem.Behav. **31**(1):75-79.
39. **Blumenthal M, Busse WR and Goldberg A (2000):** The complete commission monographs. Therapeutic guide to herbal medicines .Boston, M.A. Integrative Medicines Communication. **102**: 80-81.
40. **Gorczynska E and Wegrynowicz R (1991):** Structural and functional changes in organelles of liver cells on rat exposed to magnetic fields. Environ. Res. **55**: 188-189.
41. **Cogger VC, Muller M, Fraser R and Khan J (2004):** Effect of oxidative stress on the liver sieve. Journal of Hepatology. **41**: 370-376.
42. **Goran B, Branko J, Vesna S, Katarina P and Jelena I (2008**): Urban road-traffic noise and blood pressure and heart rate in preschool children. Environment International. **34**: 226-231.
43. **Uran SL, Caceres LG and Guelman LR (2010):** Effectsof loud noise on hippocampal and cerebellar–relatedrole of oxidative state. Behavior Brain Research. **1361**: 102-114.
44. **El Habit O, Saada H, Azab K, Abdel-Rahman M and El Malah D (2000):** The modifying effect of beta carotene on gamma radiation-induced elevation of oxidative reactions and genotoxicity in male rats. Mut. Res. **466**: 179-190.
45. **Saada H and Azab K (2001):** Role of lycopene in recovery of radiation induced injury to mammalian cellular organelles**.** Journal of Pharmazie. **56**(3): 239-240.
46. **Bunney GK (1992):** Agajanian, dopamine and norepinephrine inner- evolvement of both dopaminergic and GABAergic components, vetted cells in the ratprefrontal cortex: pharmacological differentia. Journal of Neuroscience. **49**: 857–865.
47. **Mark Pb, Bhashkar MB, Christopher L and Huangb K (2001):** Detection of pharmacologically mediated changes in cerebral activity by functional magnetic resonance imaging: the effects of sulpiride in the brain of the anaesthetised rat. Brain Research. **916**: 107–114.
48. **Braet F, Muller M, Vekeman K, Wisse E and Le DG (2003):** Antimycin A-induced defenestration in rat hepatic sinusoidal endothelial cells. Journal of Hematology. **38**: 394- 402.

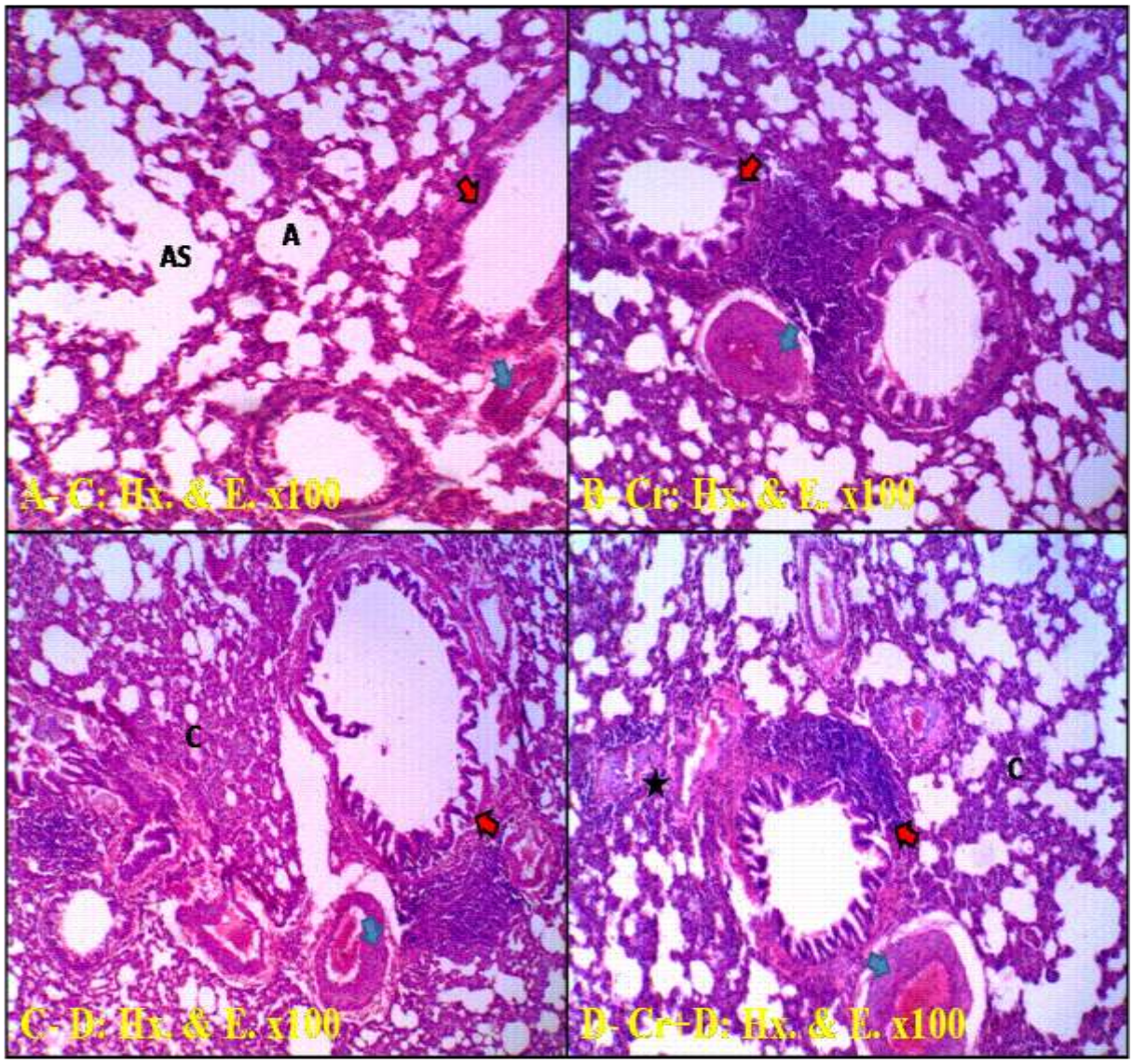

Fig. 1: A) Group 1 "**C**ontrol rats" lung shows normal architecture of alveoli (A) with thin interalveolar septa, alveolar sacs (AS), bronchiole with folded lining epithelial cells (red arrow) and normal pulmonary vessel (blue arrow). **B) Group 2 "Cr**owding exposed rat" lung shows obliteration of some alveoli with subsequent compensatory dilatation of others and thickened interalveolar septa. Numerous areas of cellular infiltration are detected in the connective tissue surrounding lung bronchioles that shows elongated and corrugated walls (red arrow). Thickened walls of the pulmonary blood vessels (blue arrow) are also detected. **C) Group 3 "D**rug exposed rat" lung shows similar findings to crowding exposed one. **D) Group 4 "Cr**owding **+ D**rug exposed rat" lung shows marked obliteration of some alveoli (c) and subsequent compensatory dilatation of others with thickened interalveolar septa. Marked thickening of bronchiole walls, peribronchiolar infiltration with inflammatory cells (red arrow) were detected. Moreover, thickened and congested pulmonary blood vessels (blue arrow) with marked perivascular infiltration (Black star) are detected (**Hx. & E. x100).**

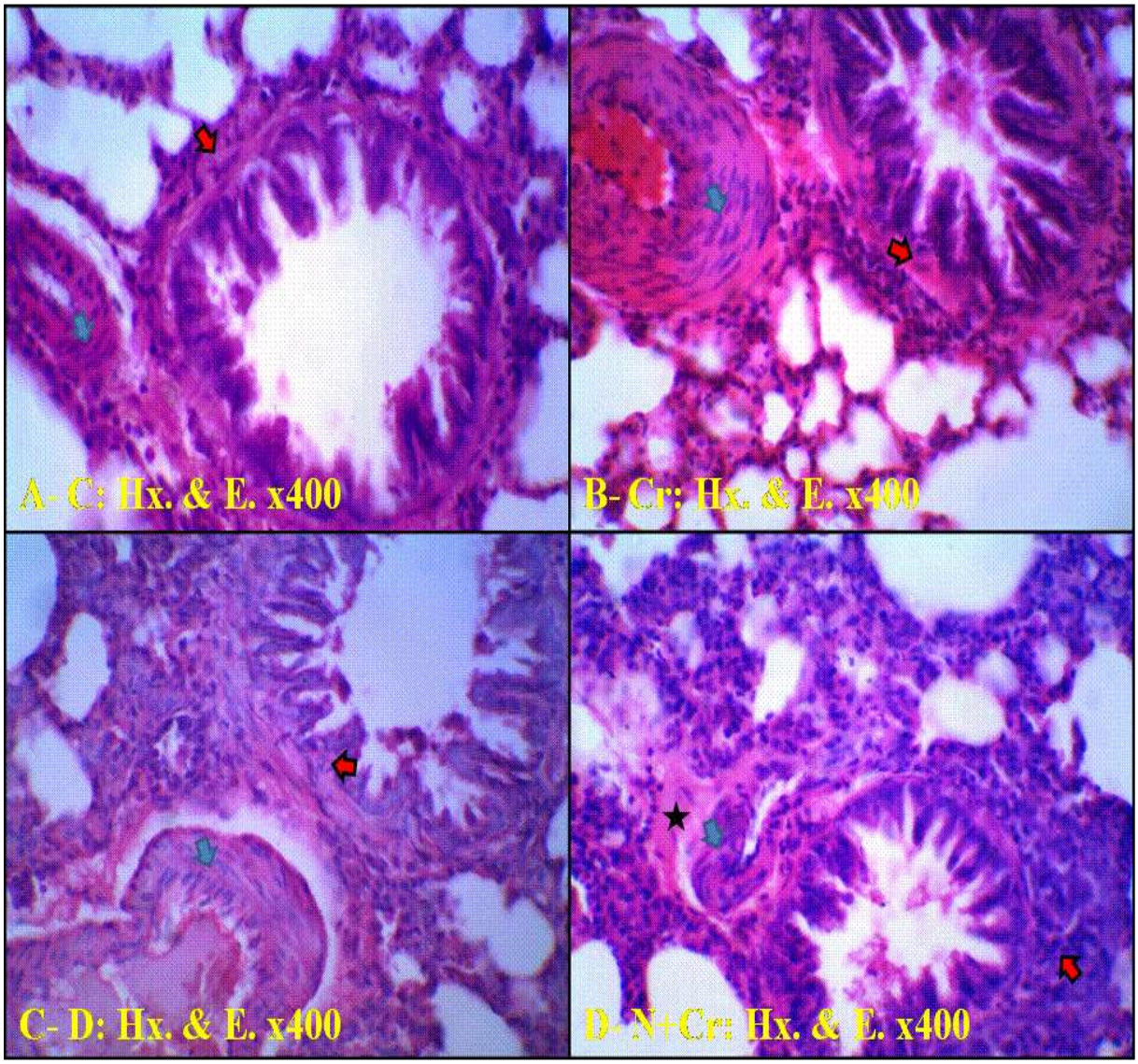

Fig. 2: A) Group 1 "**C**ontrol rats" lung shows normal architecture of alveoli (A) with thin interalveolar septa, bronchiole with highly folded columnar epithelial cells (red arrow) and normal pulmonary vessel (blue arrow). **B) Group 2 "**Crowding exposed rat" lung shows obliteration of some alveoli with subsequent compensatory dilatation of others. There is destruction in the surrounding bronchial muscle layer together with partial shedding of the mucosal lining, appearance of cell debris in the destructed bronchiole and numerous areas of inflammatory cells infiltration in connective tissue surrounding lung bronchiole (red arrow). Thickened wall of the pulmonary blood vessels (blue arrow) which contain blood cells is also detected. **C) Group 3 "D**rug exposed rat" lung shows somehow similar findings to crowding exposed one. **D) Group 4 "Cr**owding + **D**rug exposed rat" lung shows marked obliteration of some alveoli with subsequent compensatory dilatation of others and thickening of interalveolar septa. Peribronchiolar inflammatory cells infiltration is also detected (red arrow). Marked thickening of pulmonary blood vessels (blue arrow) with marked perivascular infiltration and degeneration are also detected (black star). (**Hx. & E. x400).**

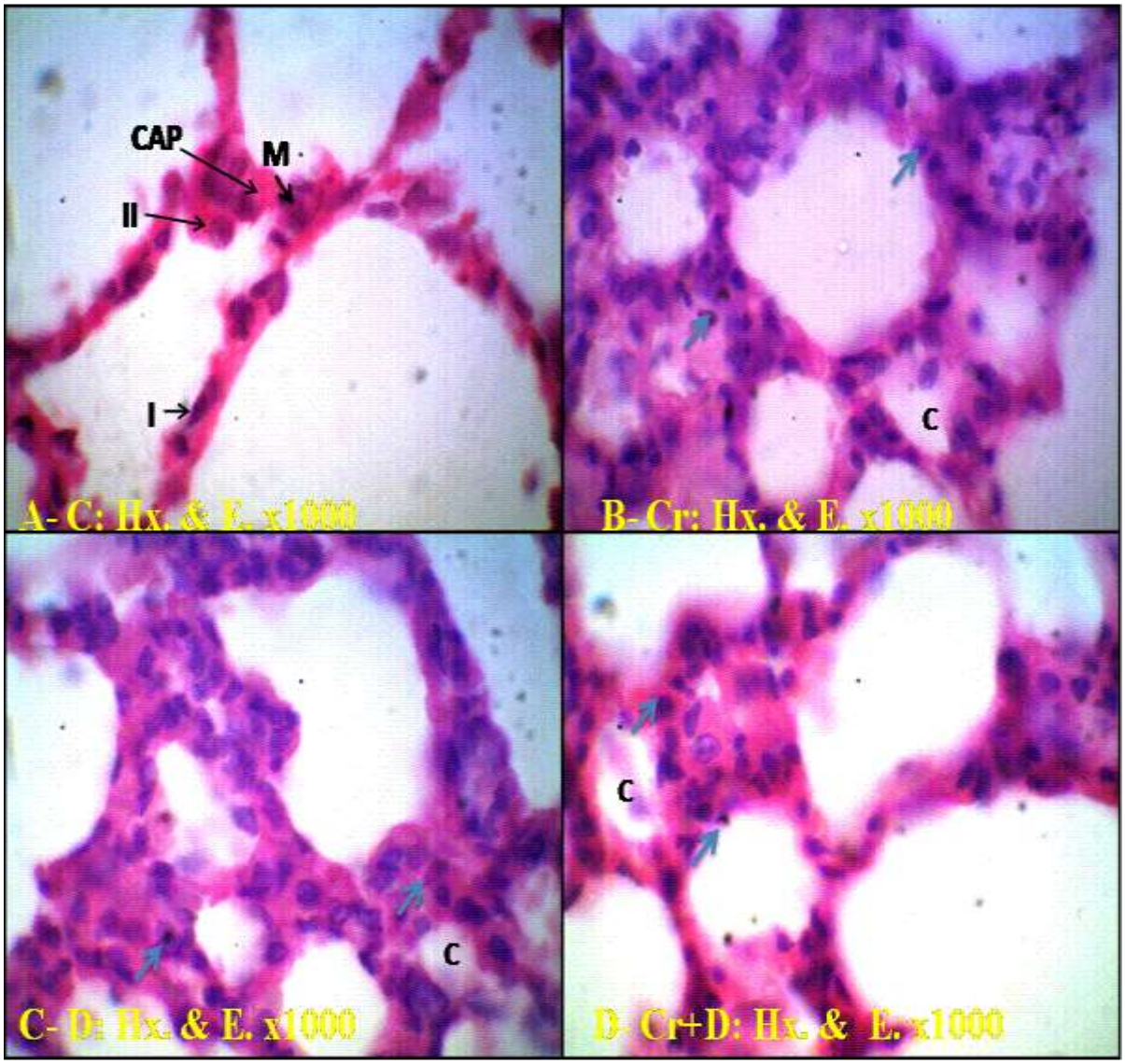

Fig. 3: A) Group 1 "**C**ontrol rats" lung shows the architecture of alveoli with thin interalveolar septa lined with type I pneumocyte (I) and type II pneumocyte (II), capillaries (CAP). Few number of macrophages (M) are also detected in the lung interstitium. **B) Group 2 "Cr**owding exposed rat" lung shows collapsed alveoli (c) with compensatory expansion of other ones, thickening of interalveolar septa with massive infiltration of inflammatory cells. Cellular apoptotic changes are also detected (blue arrows). **C) Group 3 "D**rug exposed rat" lung shows similar findings to crowding-exposed one. **D) Group 4 "Cr**owding **+ D**rug exposed rat" lung shows marked obliteration of some alveoli (c) with subsequent compensatory dilatation of others and in thickened interalveolar septa. Cellular apoptotic changes (karyolysis and pyknosis) are also detected (blue arrows). (**Hx. & E. x1000).**

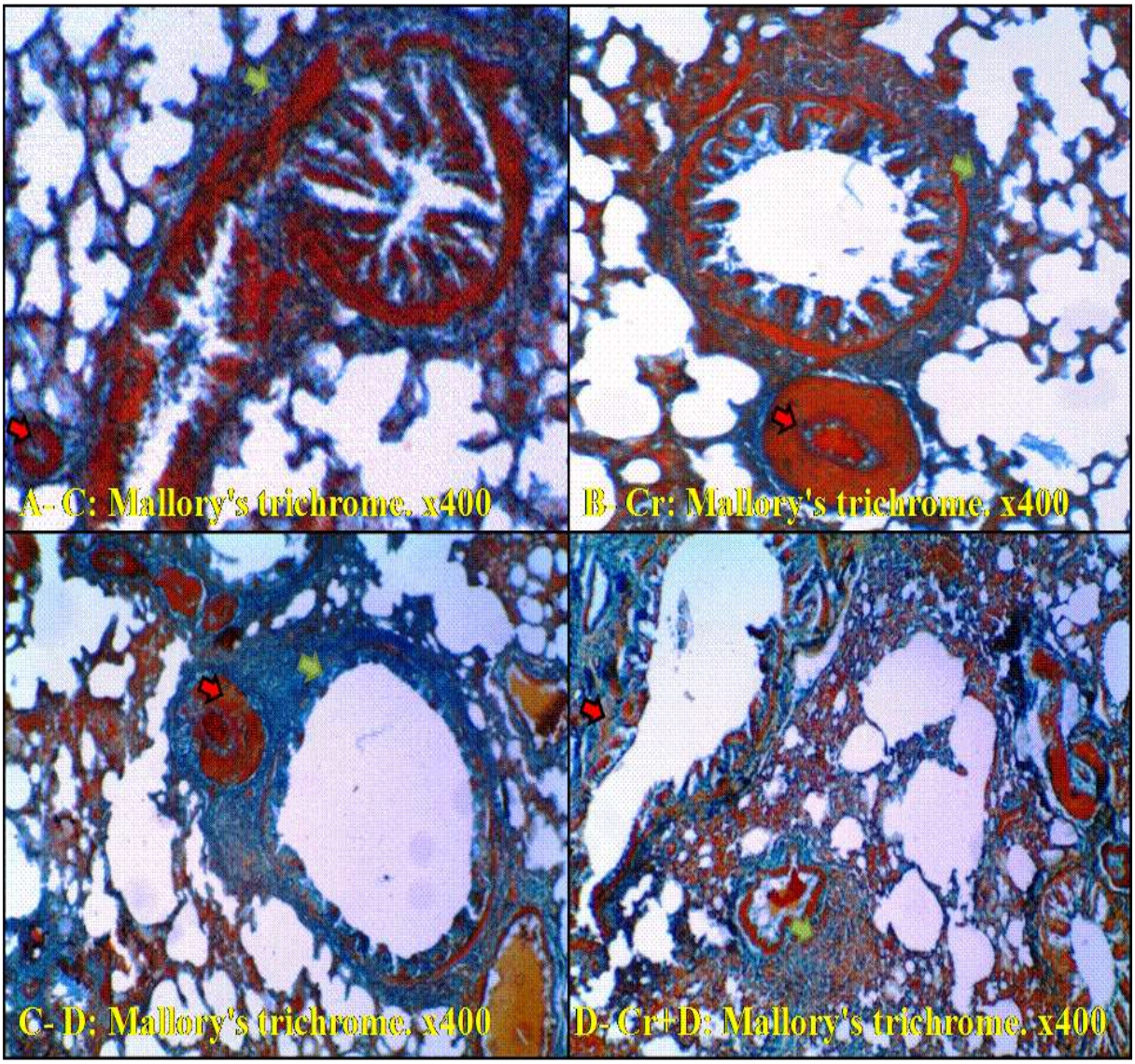

Fig. 4: A) Group 1 "**C**ontrol rats" lung shows normal distribution of collagen fibres in pulmonary interstitium around the bronchioles (green arrow), pulmonary blood vessels (red arrow), alveolar sacs and in-between alveoli. **B) Group 2 "Cr**owding exposed rat" lung shows moderate amount of collagen fibres in the bronchiole submucosa, peribronchiolar area (green arrow) and in thick interalveolar septa with cellular infiltration in interalveolar septa. Areas of cellular infiltration are observed surrounding lung bronchioles. Moderate amount of collagen fibres are detected around the blood vessels (red arrow) with moderate thickening of the blood vessels. **C) Group 3 "D**rug exposed rat" lung shows similar results to Group 2 with more collagen deposition around the bronchiole submucosa, peribronchiolar area (green arrow), in thick interalveolar septa and blood vessels (red arrow). Also, partial shedding of bronchiole mucosal lining is detected (green arrow). **D) Group 4 "Cr**owding + **D**rug exposed rat" lung shows marked amount of collagen fibres in bronchiole mucosa, submucosa (green arrow), peribronchiolar area and in thick interalveolar septa with cellular infiltration in interalveolar septa. Marked amount of collagen fibres are detected around the blood vessels with marked thickening of the blood vessels (red arrow). (**Mallory's trichrome. x400).**

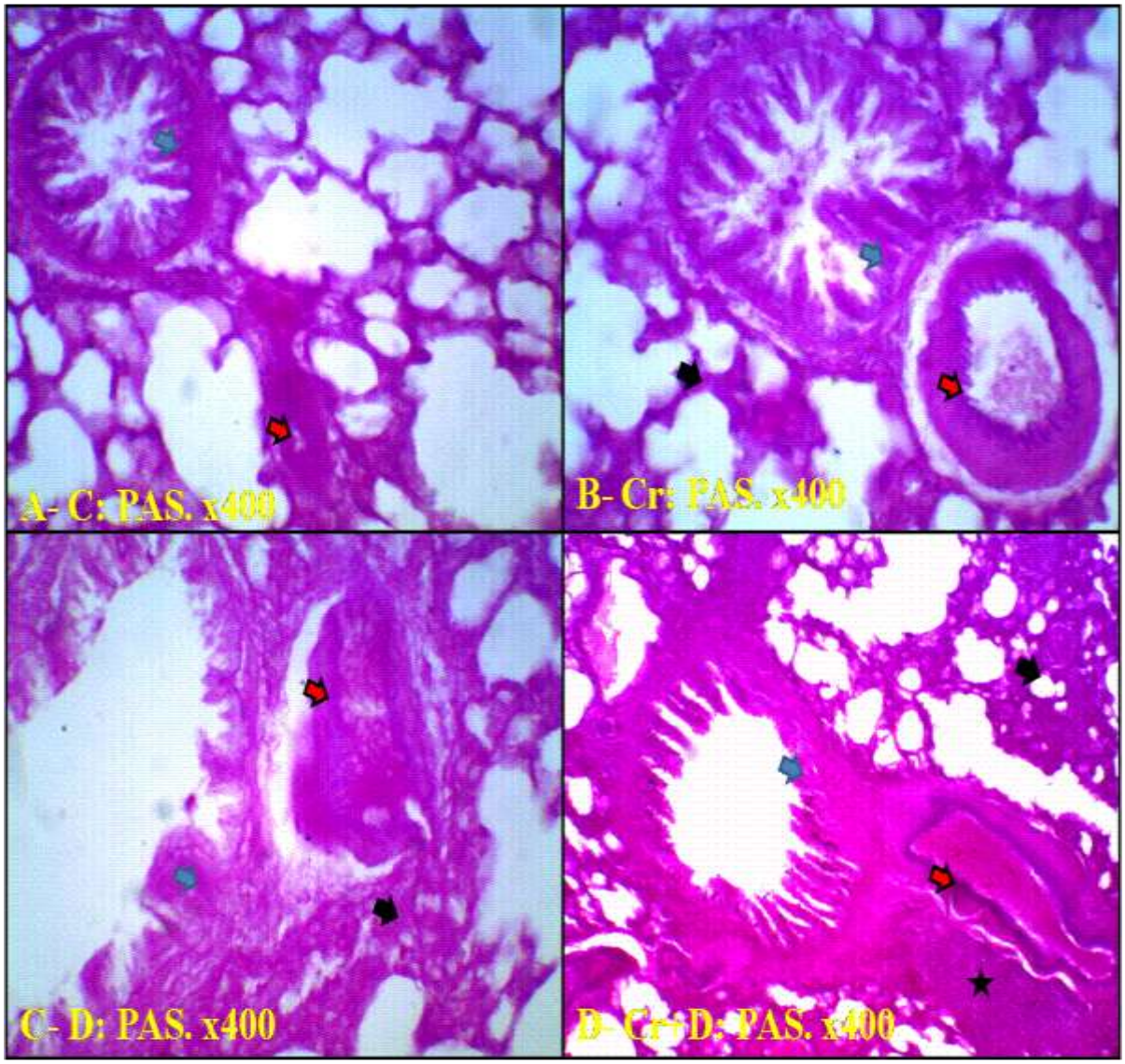

Fig. 5: A) Group 1 "**C**ontrol rats" lung shows moderate PAS reaction (magenta red) in the basal lamina of the alveolar epithelium, alveolar sacs, endothelium of pulmonary vessels (red arrows) as well as the cytoplasm of epithelium lining bronchiole (blue arrow). **B) Group 2 "Cr**owding exposed rat" lung shows strong PAS reaction in RBCs seen in the congested pulmonary vessels, in the endothelium of pulmonary vessels (red arrow), shedded bronchiole epithelial cells (blue arrow) and in sites of interstitial cellular infiltration. Strong PAS reaction in alveolar epithelium, alveolar sacs and collapsed alveoli (black arrow) are observed. **C) Group 3 "D**rug exposed rat" lung shows similar findings to crowding exposed one. However, weak PAS reaction is observed in the perivascular areas (red arrow) and collapsed alveoli (black arrow) **D) Group 4 "Cr**owding **+ D**rug exposed rat" lung shows very strong PAS reaction in endothelium of the pulmonary vessels, in the perivascular area (red arrow), and in sites of interstitial cellular infiltration (black star). Also, strong PAS reaction is observed in the bronchiole epithelial cells, peribronchiolar area (blue arrow) and the collapsed alveoli (black arrow). (**PAS. x400).**

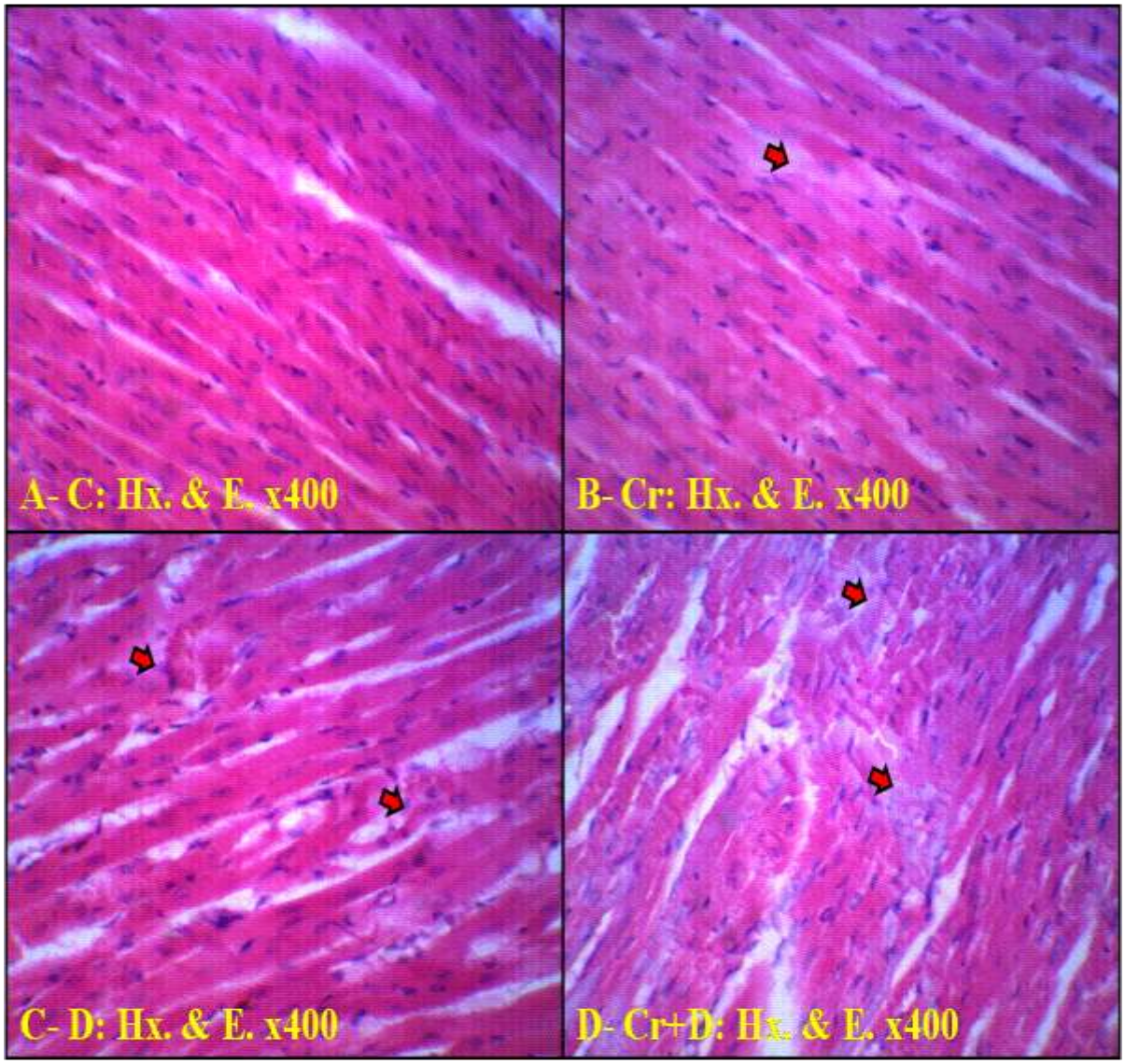

Fig. 6: A) Group 1 "**C**ontrol rats" heart shows branching and anastomosing cardiac muscle fibres with acidophilic sarcoplasm and central elongated nuclei. **B) Group 2 "Cr**owding exposed rat" heart shows some degenerative changes in myocardial fibres with numerous faintly-stained nuclei. **C) Group 3 "D**rug exposed rat" heart shows more myocardial cellular degenerative changes, widened endomysium than group 2. **D) Group 4 "Cr**owding **+ D**rug exposed rat" heart shows marked myocardial cellular degenerative changes, separation of cardiac muscle fibres with highly-widened endomysium which contains debris of degenerated myocardial muscle fibres (red arrows). **(Hx. & E. X400).**

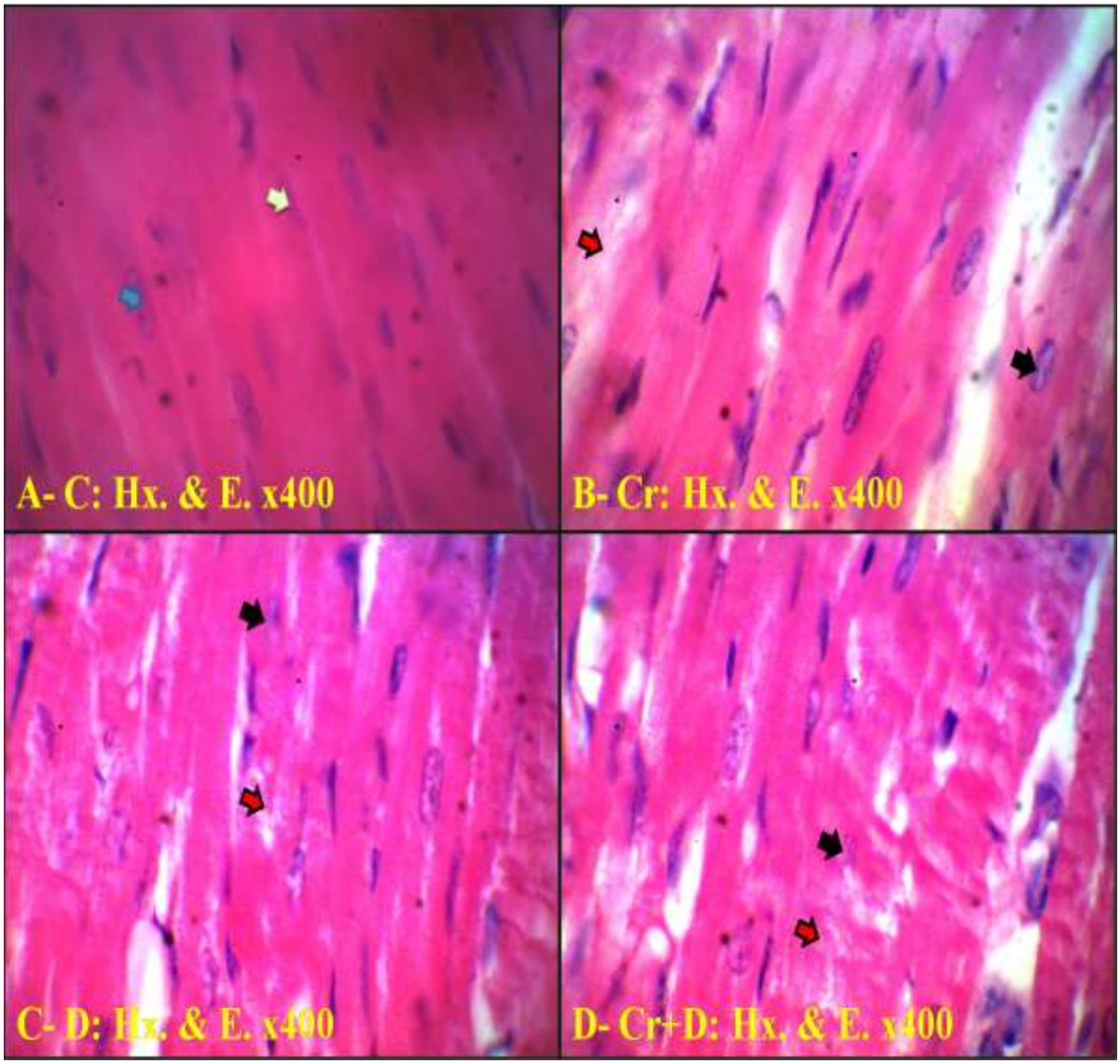

Fig. 7: A) Group 1 "**C**ontrol rats" heart shows branching and anastomosing cardiac muscle fibres with acidophilic sarcoplasm, vesicular nuclei of cardiomyocytes (blue arrow) and the nuclei of fibroblasts in the interstitium (yellow arrow). **B) Group 2 "Cr**owding exposed rat" heart shows focal areas of necrosis with vacuolated cytoplasm (red arrow) and small deeply-stained pyknotic nuclei (black arrow). **C) Group 3 "D**rug exposed rat" heart shows focal areas of necrotic fibres with vacuolated cytoplasm (red arrow) and small deeply stained pyknotic nuclei (black arrow). **D) Group 4 "Cr**owding **+ D**rug exposed rat" heart shows more necrosis (red arrow) and cellular karyolysis (black arrow) than groups 2 &3. (**Hx. & E. x1000).**

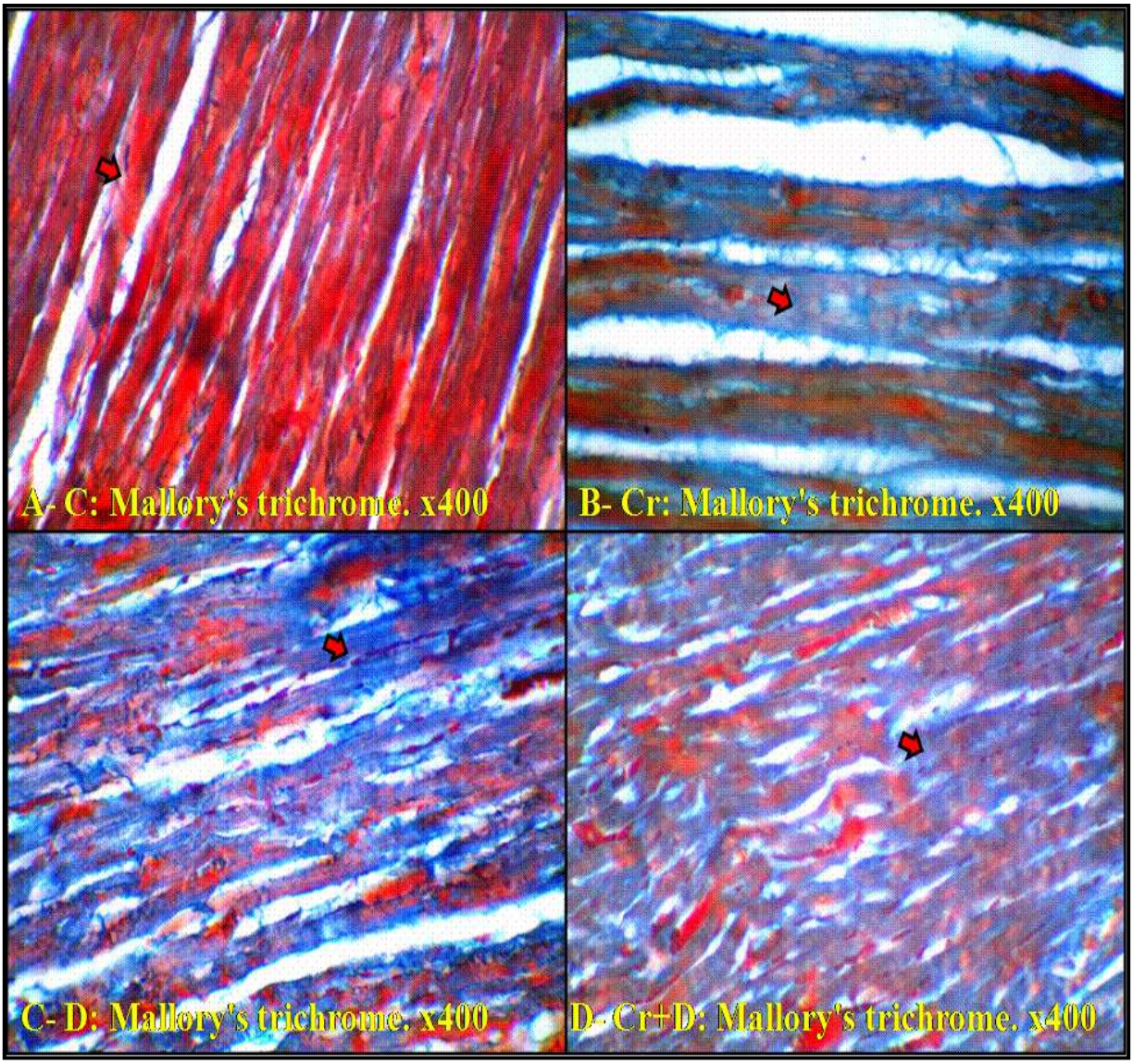

Fig. 8: **A) Group 1** "**C**ontrol rats" heart shows few collagen fibres in-between the cardiac muscle fibers (red arrow). **B) Group 2 "Cr**owding exposed rat" heart shows highly increase of the collage deposition in muscle fibres in comparison to the control group (red arrow). **C) Group 3 "D**rug exposed rat" heart shows highly increase of the collage deposition in muscle fibres in comparison to the control group (red arrow). **D) Group 4 "Cr**owding **+ D**rug exposed rat" heart shows marked increase of the collage deposition in muscle fibres in comparison to the control group (red arrow). (**Mallory's trichrome. x400).**

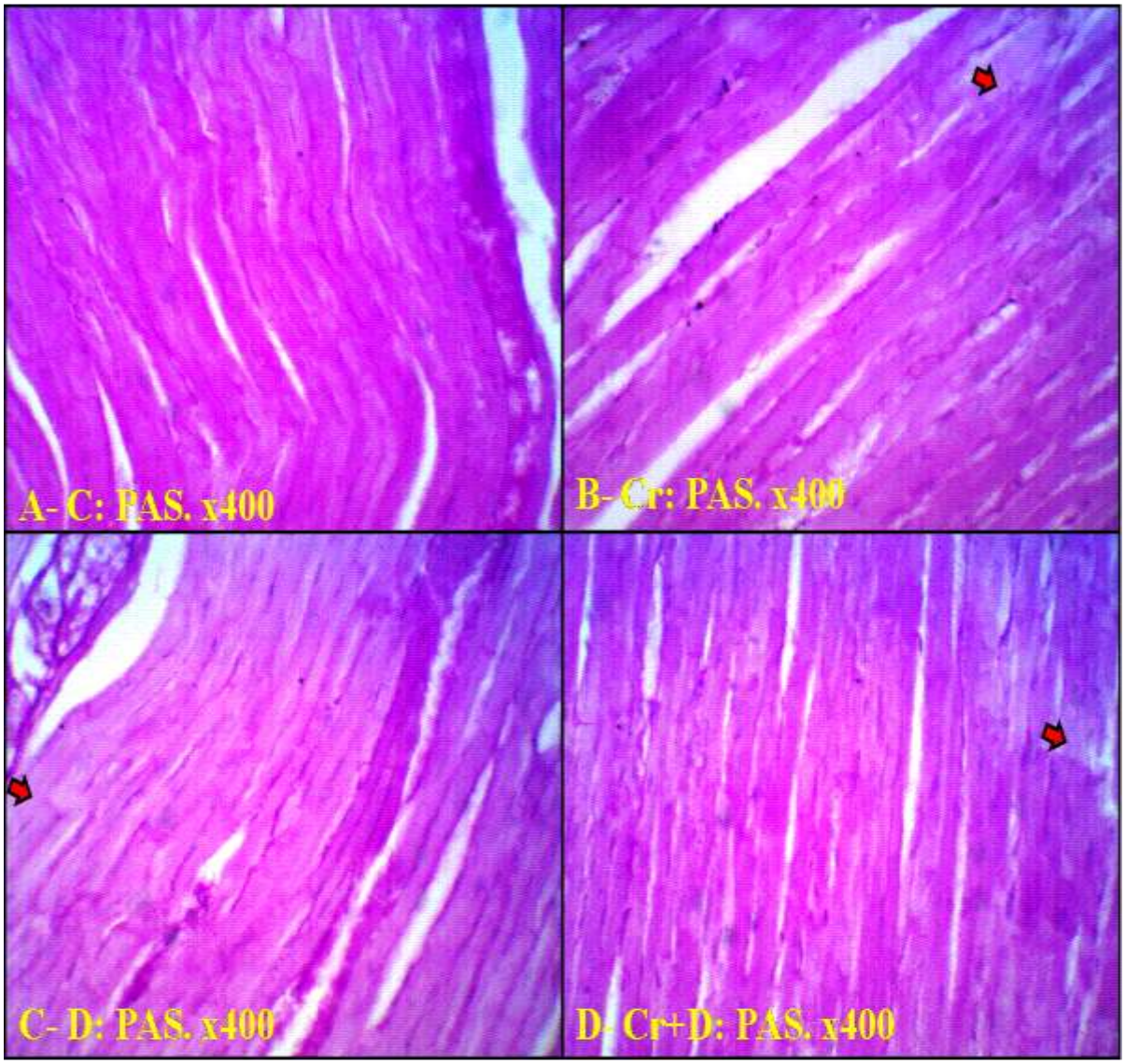

Fig. 9: A) Group 1 "**C**ontrol rats" heart shows normal polysaccharides content (normal distribution of PAS +ve materials) in the cardiac myocytes. **B) Group 2 "Cr**owding exposed rat" heart shows focal areas of poorly-stained (focal areas of decreased affinity of PAS stain) cardiac myocytes (red arrow). **C) Group 3 "D**rug exposed rat" heart shows poorly-stained (focal areas of decreased affinity of PAS stain) cardiac myocytes (red arrow). **D) Group 4 "Cr**owding **+ D**rug exposed rat" heart shows poorly-stained (focal areas of decreased affinity of PAS stain) cardiac myocytes (red arrow). (**PAS. x400).**

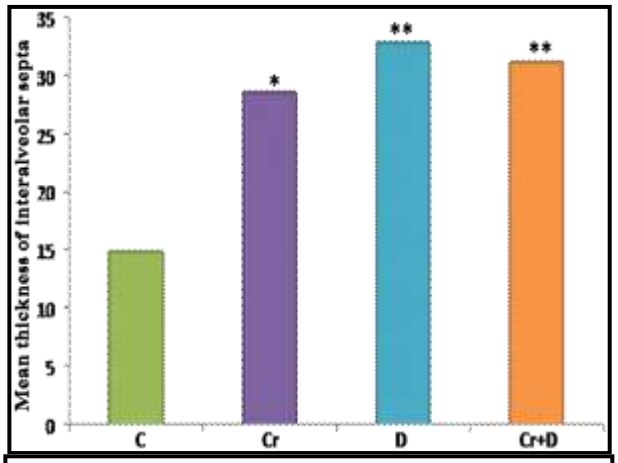

Fig. 10: The mean thickness of the interalveolar septa in lungs of the different groups of the study in comparison to the control group.

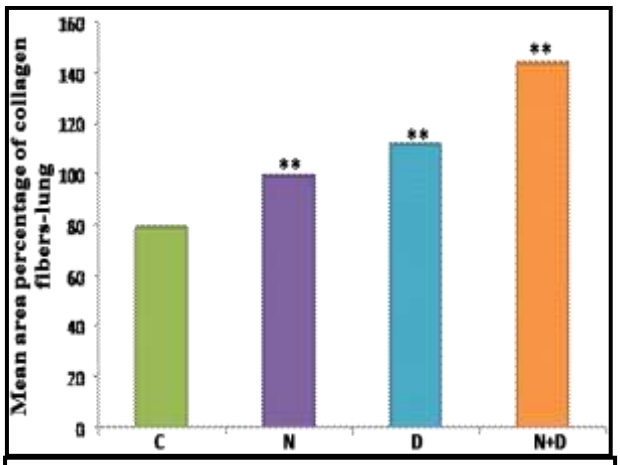

Fig. 11: The mean area percentage of the collagen fibers in lungs of the different groups of the study in comparison to the control group.

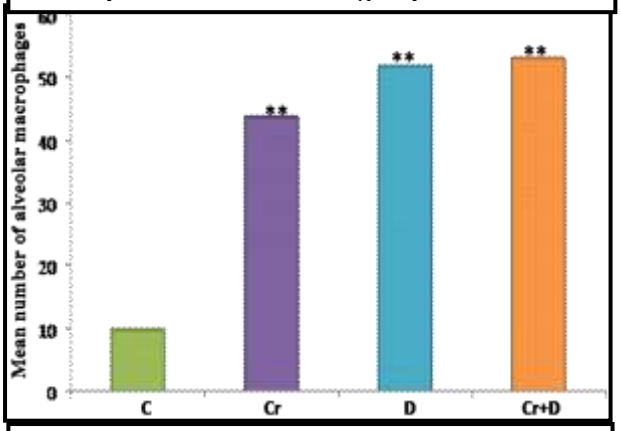

Fig. 12: The mean number of the alveolar macrophages in lungs of the different groups of the study in comparison to the control group.

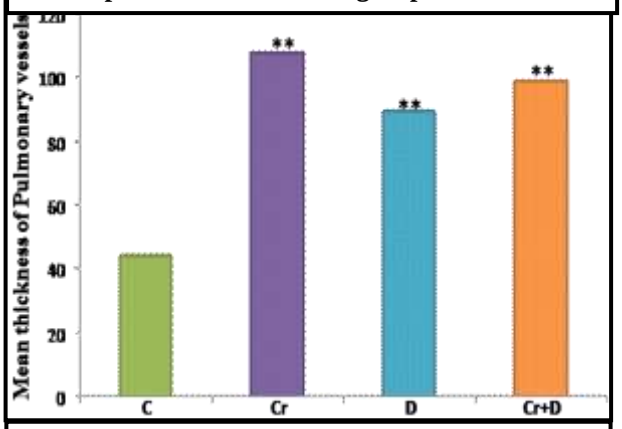

Fig. 13: The mean thickness of the pulmonary vessels in lungs of the different groups of the study in comparison to the control group.

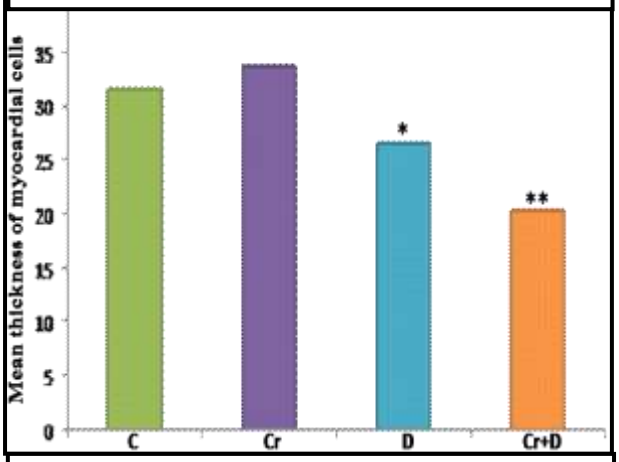

Fig. 14: The mean thickness of the cardiac myocytes of the different groups of the study in comparison to the control group.

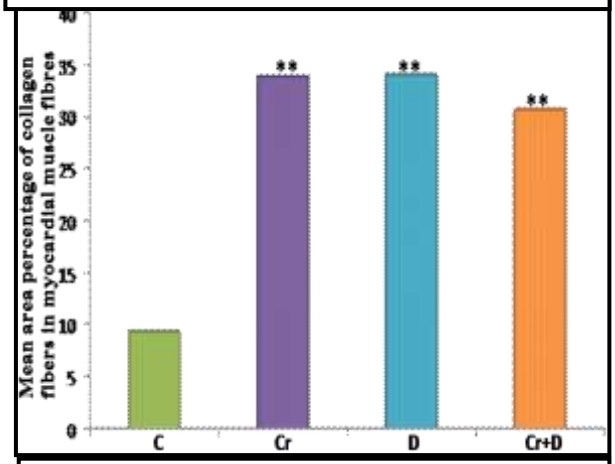

Fig. 15: The mean area percentage of the collagen fibres in the cardiac myocytes of the different groups of the study in comparison to the control group.

Parameters / Study Group	Thickness of the interalveolar speta	Area percentage of collagen fibres in the lung alveoli	Number of the alveolar macrophages	Thickness of the pulmonary vessels	Thickness of the myocardial muscle fibres	Area percentage of collagen fibres in the myocardial muscle fibres
Group 1 (C)	**14.86± 3.53**	**79.21± 29.1**	**10± 1.58**	**44.37± 8.26**	**31.68± 3.87**	**9.37± 2.32**
Group 2 (Cr)	**28.57± 8.52***	**99.54± 35.47***	**43.78± 1.86****	**107.83± 18.39****	**33.63± 5.57**	**33.92± 2.72****
Group 3 (D)	**32.91± 8.35****	**111.75± 43.0****	**51.89± 2.85****	**89.42± 11.62****	**26.55± 2.26***	**33.98± 2.96****
Group 4 (Cr + D)	**31.19± 7.15****	**144.05± 29.22****	**53.22± 2.33****	**98.92± 16.16****	**20.36± 2.99****	**30.81± 3.34****

Table (1): Thickness of interalveolar septa, number of alveolar macrophages, percentage of collagen fibres in the lung alveoli, thickness of the pulmonary vessels, thickness of the myocardial muscle fibres and percentage of collagen fibres in the myocardial muscle fibres of the different groups of the study expressed as mean ± SD.

*Significantly different from the control group ($P < 0.05$).
**Significantly different from the control group ($P < 0.001$).